NASA/TM–20240012459

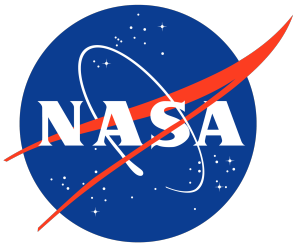

Dynamic Mechanical Analysis of Post-Cured Bismaleimide Resins for Composite-Overwrapped Combustion Chambers Cycled From Cryogenic to High Temperatures

(Christopher Stelter)
(NASA Langley Research Center, Hampton, VA)

(Cheol Park)
(NASA Langley Research Center, Hampton, VA)
(Sang-Hyon Chu)
(NASA Langley Research Center, Hampton, VA)
(Tyler Hudson)
(NASA Langley Research Center, Hampton, VA)

October 2024

NASA STI Program Report Series

Since its founding, NASA has been dedicated to the advancement of aeronautics and space science. The NASA scientific and technical information (STI) program plays a key part in helping NASA maintain this important role.

The NASA STI Program operates under the auspices of the Agency Chief Information Officer. It collects, organizes, provides for archiving, and disseminates NASA's STI. The NASA STI Program provides access to the NTRS Registered and its public interface, the NASA Technical Report Server, thus providing one of the largest collections of aeronautical and space science STI in the world. Results are published in both non-NASA channels and by NASA in the NASA STI Report Series, which includes the following report types:

- TECHNICAL PUBLICATION. Reports of completed research or a major significant phase of research that present the results of NASA programs and include extensive data or theoretical analysis. Includes compilations of significant scientific and technical data and information deemed to be of continuing reference value. NASA counterpart of peer-reviewed formal professional papers, but having less stringent limitations on manuscript length and extent of graphic presentations.
- TECHNICAL MEMORANDUM. Scientific and technical findings that are preliminary or of specialized interest, e.g., quick release reports, working papers, and bibliographies that contain minimal annotation. Does not contain extensive analysis.
- CONTRACTOR REPORT. Scientific and technical findings by NASA-sponsored contractors and grantees.
- CONFERENCE PUBLICATION. Collected papers from scientific and technical conferences, symposia, seminars, or other meetings sponsored or co-sponsored by NASA.
- SPECIAL PUBLICATION. Scientific, technical, or historical information from NASA programs, projects, and missions, often concerned with subjects having substantial public interest.
- TECHNICAL TRANSLATION. English-language translations of foreign scientific and technical material pertinent to NASA's mission.

Specialized services also include organizing and publishing research results, distributing specialized research announcements and feeds, providing information desk and personal search support, and enabling data exchange services.

For more information about the NASA STI Program, see the following:

- Access the NASA STI program home page at `http://www.sti.nasa.gov`
- Help desk contact information: `https://www.sti.nasa.gov/sti-contact-form/` and select the "General" help request type.

NASA/TM–20240012459

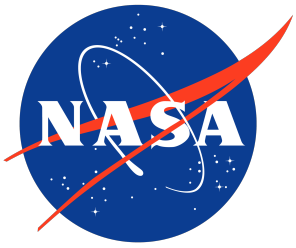

Dynamic Mechanical Analysis of Post-Cured Bismaleimide Resins for Composite-Overwrapped Combustion Chambers Cycled From Cryogenic to High Temperatures

(Christopher Stelter)
(NASA Langley Research Center, Hampton, VA)

(Cheol Park)
(NASA Langley Research Center, Hampton, VA)
(Sang-Hyon Chu)
(NASA Langley Research Center, Hampton, VA)
(Tyler Hudson)
(NASA Langley Research Center, Hampton, VA)

National Aeronautics and
Space Administration

Langley Research Center
Hampton, Virginia 23681-2199

October 2024

Acknowledgments

The authors would like to express their appreciation to the Space Technology Mission Directorate (STMD), Game Changing Development program, Rapid Analysis and Manufacturing Propulsion Technology (RAMPT) project, for their support.

Available from:

NASA STI Program / Mail Stop 150
NASA Langley Research Center
Hampton, VA 23681-2199

Abstract

In support of the Rapid Analysis and Manufacturing Propulsion Technology (RAMPT) project, samples made of polybismaleimide (BMI) resin were made and tested under cryogenic conditions. Neat resin samples were tested for multiple cycles, from high temperature (300°C) to cryogenic temperature (-150°C), to replicate the conditions a rocket engine assembly would experience in a test campaign and in operation. To increase the glass transition temperature (and thus mechanical stability), samples were exposed to different post-cure temperatures and were tested using a dynamic mechanical analysis (DMA) instrument. Consistent with expectations, the BMI samples post-cured at higher temperatures generally resulted in higher storage modulus under high temperature test conditions but at the expense of storage modulus values at low temperature test conditions.

1 Introduction

The goal of the Rapid Analysis and Manufacturing Propulsion Technology (RAMPT) project under NASA Game Changing Development (GCD) program was to mature novel design and processing technologies to improve performance of regeneratively-cooled thrust chamber assemblies (TCA) fabricated at greater scale, significantly reduced cost, and with higher performance [1]. The RAMPT project utilized carbon fiber reinforced polymer (CFRP) matrix composite overwraps (particularly in the circumferential direction, the principle stress in a cylindrical pressure vessel [2], such as a rocket combustion chamber) to provide mass efficient reinforcement over additively manufactured metallic rocket chambers. As carbon fiber has a higher strength to weight ratio than the metallic alloys used in rocket chamber construction, such overwraps could enable engines with a higher thrust to weight ratio (either through weight reduction or increased chamber pressure [3]) and reduce the manufacturing times compared with purely metal additive manufacturing. Carbon fiber composite overwrapped rocket engines have been featured in several experimental ablatively cooled rocket engines, such as those made by Scorpius Space Launch Company [4]. However, regeneratively cooled liquid rocket engines, which can achieve higher performance, typically experience a wide range of temperature extremes during operation. Rocket propellants, which flow through the metallic rocket chamber walls for regenerative cooling—such as liquid methane, liquid hydrogen, and liquid oxygen—are deeply cryogenic (as low as 20 Kelvin). However, at the end of a rocket burn or where there is not sufficient regenerative cooling, parts of the engine can experience high temperatures as well (350°C or beyond). These conditions pose a challenge to the polymer composite overwraps which can become brittle at low temperatures and soften at high temperatures. Therefore, an experimental campaign to examine the suitability of polymeric resins and various processing procedures was performed. This work describes some of the results of this campaign, specifically examining polybismaleimide (BMI) neat resin that had been post-cured at various temperatures in order to increase its use temperature as measured by the change in its glass transition temperature (T_g) and overall storage modulus as a function of

temperature.

Additionally, liquid rocket engines such as those envisioned to use the technology developed under RAMPT project typically are required to undergo many firings, both as part of the certification process, for nominal operations, and with margins to allow aborted lift-off capability. This is especially true during development. A liquid rocket engine may undergo one or many certification firings on a test stand before being integrated on the rocket vehicle, where it may undergo more integrated test firings followed by a launch attempt. During a nominal mission, there may also be multiple engine firings, especially for upper stage engines. Finally, many liquid rocket engines are designed to be reused for multiple missions, potentially certified for dozens or even hundreds of mission cycles. Therefore, this work also explores the effect of multiple thermal cycles on the T_g and storage modulus as a function of temperature.A dynamic mechanical analysis (DMA) instrument was used to perform these measurements [5], [6]. These data are then analyzed using repeatable methods described within.

2 Experimental

2.1 BMI Resin

Cycom® 5250-4 bismaleimide resin, a thermosetting polyimide, was purchased from Syensqo® (formerly Solvay®, formerly Cytec® Industries, Cycom® 5250-4). Cycom® 5250-4 is a toughened BMI resin with the following three components in a 6:4:5 molar mixture: 4,4'-Bismaleimidodiphenylmethane (BMPM), BMI-1,3-tolyl, and o,o'-diallylbisphenol A (DABPA) [7]. The chemical structures of the three components of the BMI resin are shown in Figure 1. BMI resin forms an aromatic backbone, giving it excellent stiffness and temperature stability while retaining toughness.

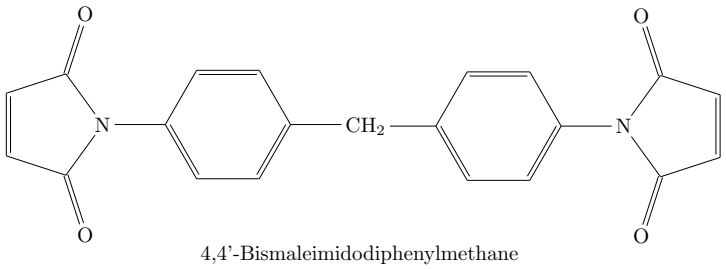

4,4'-Bismaleimidodiphenylmethane

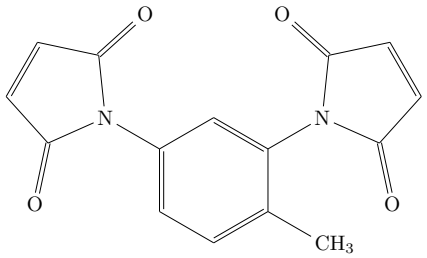

BMI-1,3-tolyl

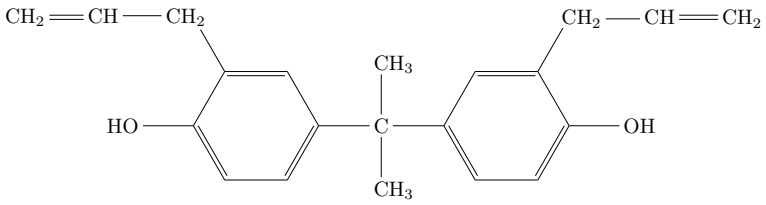

o,o'-Diallylbisphenol A

Figure 1: Components of Cycom® 5250-4 resin.

The cure process of BMI resins such as Cycom® 5250-4 is relatively complex. Exploration of the details of this chemical process is beyond the scope of this paper. However, prior research shows that extended cure times can affect their material properties, including causing degradation [8]. In general, increased cure time and temperature should increase the amount of cross-linking which should increase the glass transition temperature, but at the same time, high temperatures for long periods may start degrading the polymer through chain scissions (which would be expected to lower the overall modulus) and eventually result in decomposition.

2.2 Sample Preparation

After the BMI resin was degassed, samples were cast in a mold and cured according to the manufacturer's recommended cure cycles shown in Figure 2. A higher post-cure temperature (260°C) than typical was used in an effort to improve the high temperature performance of the resin. A summary of the sample preparation procedure is shown in Figure 3.

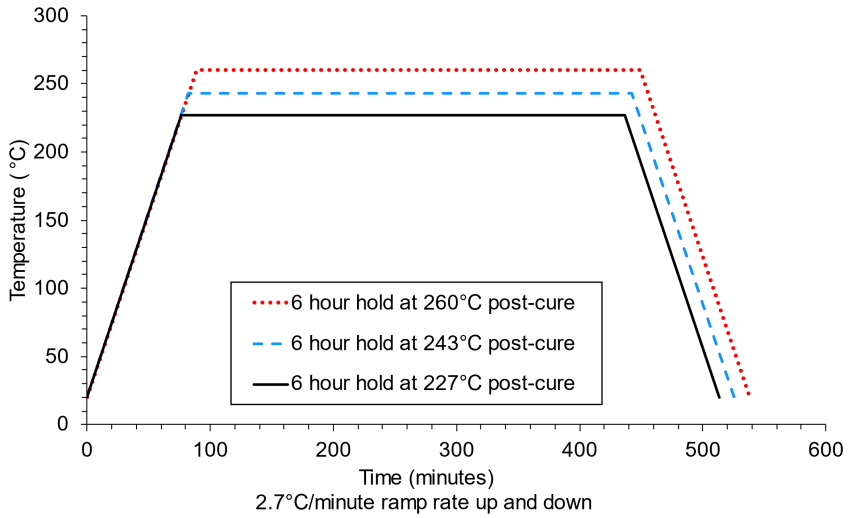

a)

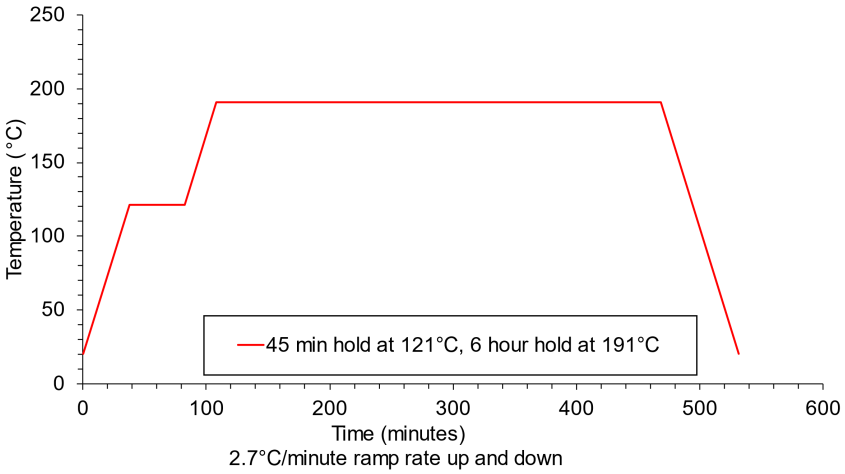

b)

Figure 2: The standard cure cycle (a) and the post-cure cycle (b) for Cycom 5250-4 resin, respectively.

Stainless steel blocks were cleaned and then treated with Zyvax® mold release agent. A 150 mm by 150 mm mold was assembled from the blocks with a 50-mm-high perimeter wall. Gauge blocks (5 mm) were placed in the four corners of the mold to keep the sample thickness uniform during the cure cycle. Sufficient resin thawed at 66°C was weighed and placed into the mold. The assembly was then placed in a vacuum oven and degassed for 16 hours at 50°C. Through process development and experimentation, it was found that a 50-mm-high wall ensures the

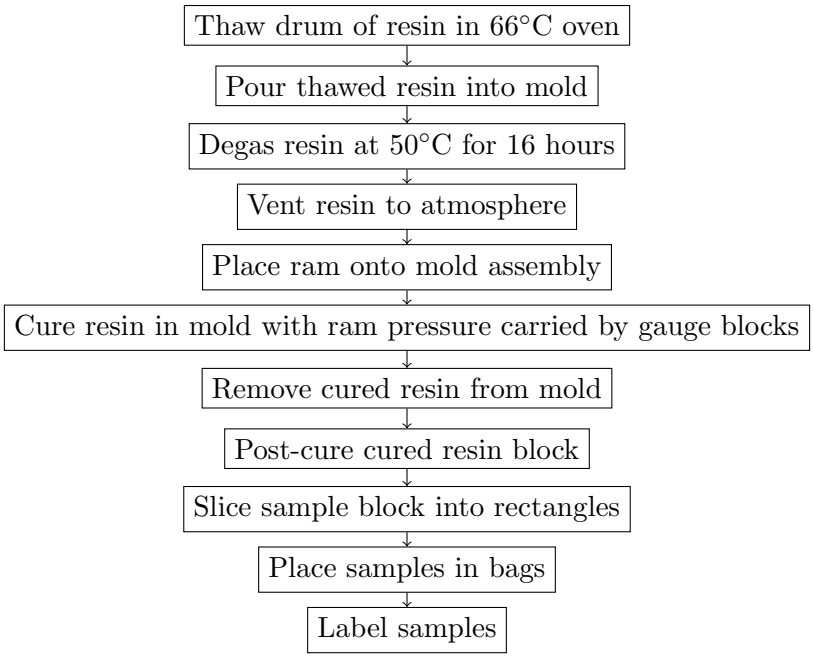

Figure 3: Basic steps for the preparation of neat resin samples.

resin does not overflow while degassing, making it unnecessary to vent the oven regularly to collapse the bubbles. After degassing, a ram was placed on top of the mold assembly in a press with minimal but sufficient pressure to ensure the ram was seated firmly on the gauge blocks. The resin was cured according to manufacturing specifications: the sample block was heated at a ramp rate of 2.7°C/min up to 121°C and held for 45 minutes followed by 191°C at the same rate and held for six hours, and finally ramping down to room temperature at the same rate of 2.7°C/min. The sample block was then de-molded and placed in an oven for a free standing post-cure procedure. For the post-cure treatment, three different temperature conditions were used for six hours (with a 2.7°C/min ramp rate up and down): 227°C, 243°C, and 260°C. For the 227°C and 243°C post-cure samples, the same sample block was used but it was first cut in half between the standard cure and post-cure treatment. The post-cured resin blocks were then cut into rectangular prisms, with dimensions on average of about 12.5 mm width, 4.5 mm thickness, and around 60 mm length. The gauge length of the test was fixed by the 3-point-bend fixture of the DMA system, which was 50 mm.

2.3 Dynamic Mechanical Analysis (DMA)

2.3.1 Background on DMA Testing

DMA is a technique for measuring the stiffness response of a material to a periodic changing input force, often varying as a function of time, temperature, and frequency. The dynamic storage and loss moduli can be found and plotted over a given temperature range. The TA Instruments® Q800 DMA instrument was used

for the current experiments. The TA Instruments® Q800 includes an environmental chamber which can be heated electrically as well as automatically cooled by the addition of cryogenic nitrogen gas from a dewar attached to the instrument called the Gas Cooling Accessory (GCA). The GCA dewar has a capacity of 50 liters and at the end of a cycle can be filled up on command from a much larger mobile dewar or other liquid nitrogen source provided the liquid nitrogen is pressurized to approximately 70 kPa to 150 kPa gauge pressure. As the mobile dewar may have over 200 liters of liquid nitrogen, this enables uninterrupted experimental runs that would not be feasible using the smaller instrument dewar alone. The testing mode initially used was the 3-point-bend with rolling contacts. Rolling contacts were used in an attempt to avoid the variation in sample stress that can occur when clamping fixtures were used. The samples cured at different conditions were tested from -150°C to 350°C at a heating rate of 5°C/min to collect data at three different frequencies: 1 Hz, 10 Hz, and 50 Hz. There are frequency dependent effects on measured Tg, but these were found to be only on the order of 1 to 2°C for our resin samples, as in Figure A1. Data collected at a reasonable ramp rate (5°C per minute) for the 1Hz case, although acceptable for storage modulus, was found to be poor for loss modulus and tan δ, as shown in Figure A1. Lower frequencies are preferred (as these are closest to the static loading case), therefore it was determined that a single 10 Hz frequency is sufficient.

After running some temperature versus modulus tests with the DMA instrument, it was decided to test the material effects of thermal cycling under DMA testing on the neat resin samples in order to characterize the thermal cycling the resin would experience during a typical liquid rocket engine lifetime, as discussed in the Introduction. It was expected that the repeated excursions to high temperature would have an effect similar to that of an extended post-cure cycle. The same procedure was followed as in the single-cycle tests, but the sample was left in the DMA machine and the temperature brought first to room temperature and then back down to cryogenic temperatures before the ramp up to high temperatures.

A constant strain of 0.05% was applied for thermal cycling tests; 10 cycling tests per sample were run continuously.

3 Results

The storage modulus as a function of temperature when tested at 10 Hz by DMA using three different post-cure conditions is shown in Figure 4. The graph was analyzed to find the onset glass transition temperature, and the intercept points shown in that graph correspond to the measured glass transition temperature onset for each of the three post-cure conditions. All three post-cure samples started to exhibit similar high modulus above 7000 MPa at low temperatures (-150°C) and decreased in modulus monotonously as temperature increased until the glass transition temperatures, and then rapidly decreased down to approximately 1000 MPa. There are secondary transitions in between –100°C and –50°C for all three resin samples, which might be related to the toughened nature of these BMI polymers. The modulus reduced faster for the higher post-cure temperature conditions, consistent with expectations

of additional chain scissions (higher temperatures may cause more polymer chain scissions, reducing modulus). Higher post-cure temperature, however, increased the onset glass transition temperature, delaying the dramatic drop in modulus seen at 260°C and higher. At low temperatures, the lower post-cure temperature conditions had the greater modulus (7360 MPa at -150°C for 227°C post-cure) but at very high temperatures (such as near the T_g), the post-cure processes at higher temperatures delayed the drastic drop of the sample moduli from 260°C to 300°C.

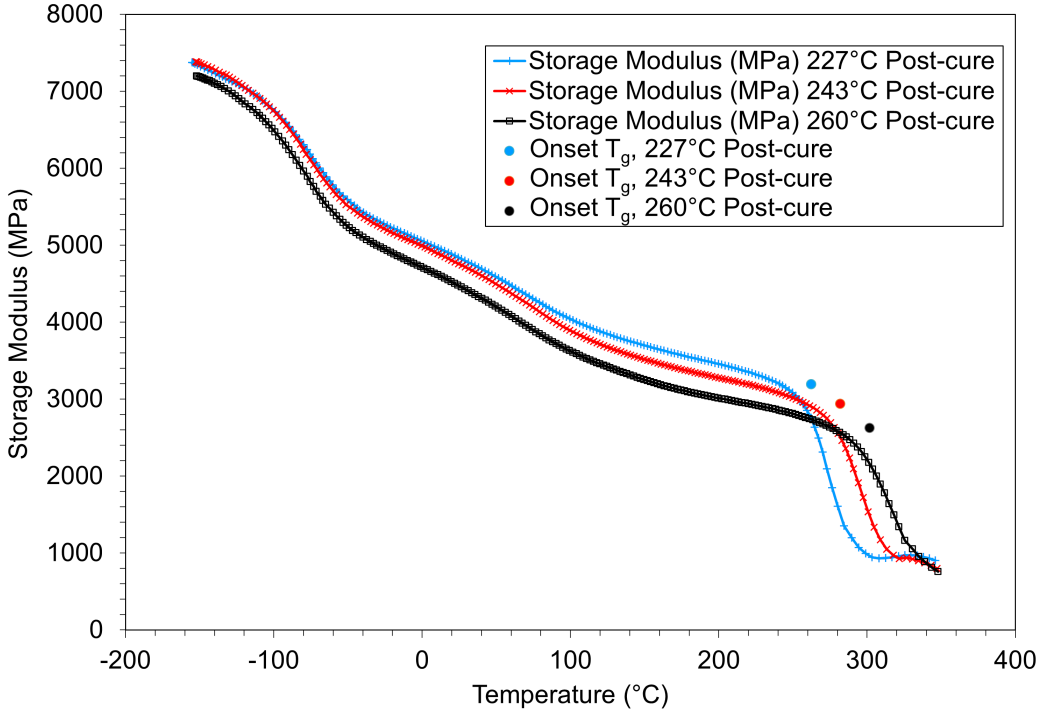

Figure 4: BMI storage modulus versus temperature using 10 Hz DMA at 5°C/min ramp rate. Colored dots indicate curve tangent intercept points used to algorithmically determine glass transition temperature.

The measured onset glass transition temperatures (note: the onset temperature is the low temperature where the glass transition region starts) are shown in Table 1 determined by both an automated and a manual measurement method, as described in Appendix A. The glass transition temperature of the BMI increased by about 30°C by raising the post-cure temperature, which extends the use temperature higher. The data from Table 1, as well as the manufacturer recommended post-cure temperature versus desired T_g, is plotted in Figure 5. For the chosen post-cure temperatures, a linear relationship was observed between post-cure temperature and onset T_g. The linear trend is such that increasing the post-cure temperature by about 1°C increase the onset T_g by about 1.2°C. The measured data is offset from the manufacturer's figures by about 15 to 20°C in the post-cure temperature axis, however the slope is similar. The reason for the 15 to 20°C discrepancy in T_g is

Post-cure Temperature (°C)	Resultant onset T_g (°C) (automated)	Resultant onset T_g (°C) (manual)
226.7	262.5	263.7
243.3	282.0	283.3
260.0	301.7	303.8

Table 1: Comparison of results from automated determination of glass transition temperature and manual determination, using the slope-tangent-intercept method.

unknown but it may be due to a difference in how the T_g is defined. The measured data uses the onset T_g from the storage modulus curve as in ASTM D7028 [5] whereas the manufacturer provided data does not specify which definition of T_g is used. This is approximately the expected difference if the manufacturer's values of T_g had used the peak loss modulus method, as described in IEC 61006:2004 [9].

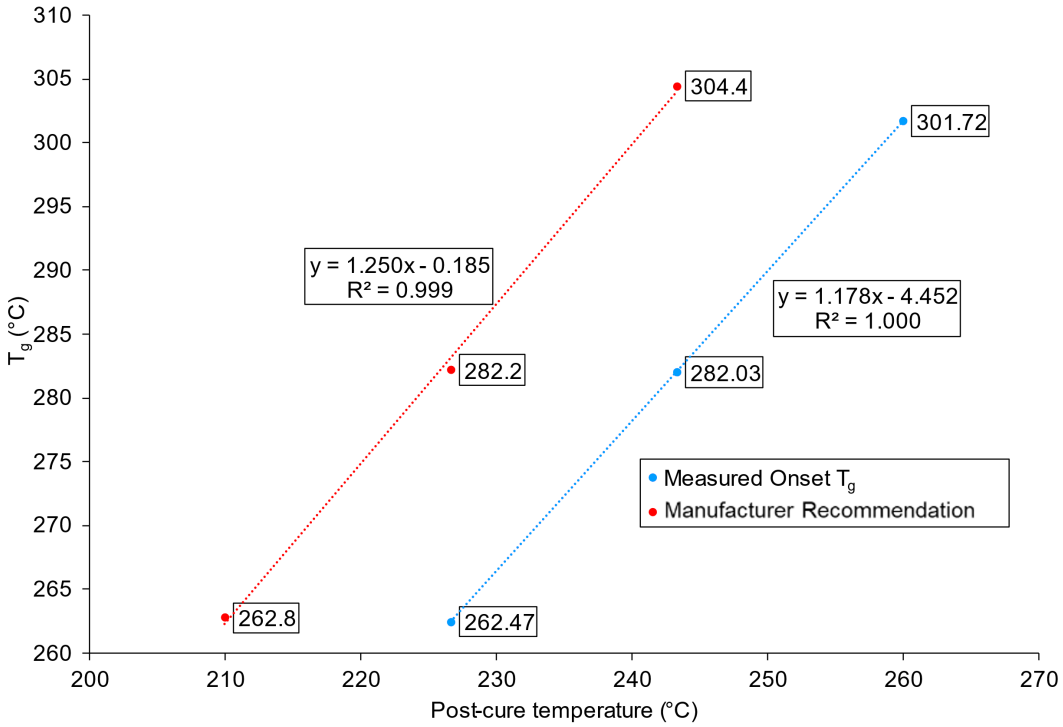

Figure 5: Comparison of the measured onset glass transition temperature with the manufacturer recommended post-cure conditions for achieving that glass transition temperature.

3.1 Effect of Cure Condition on Neat Resin Modulus.

The storage moduli collected at four different test temperatures for each post-cure temperature condition as shown in Figure 4 is summarized in Figure 6. Treating samples at higher post cure temperature increased the sample moduli at 300°C

significantly, while decreasing the moduli at the other temperatures slightly.

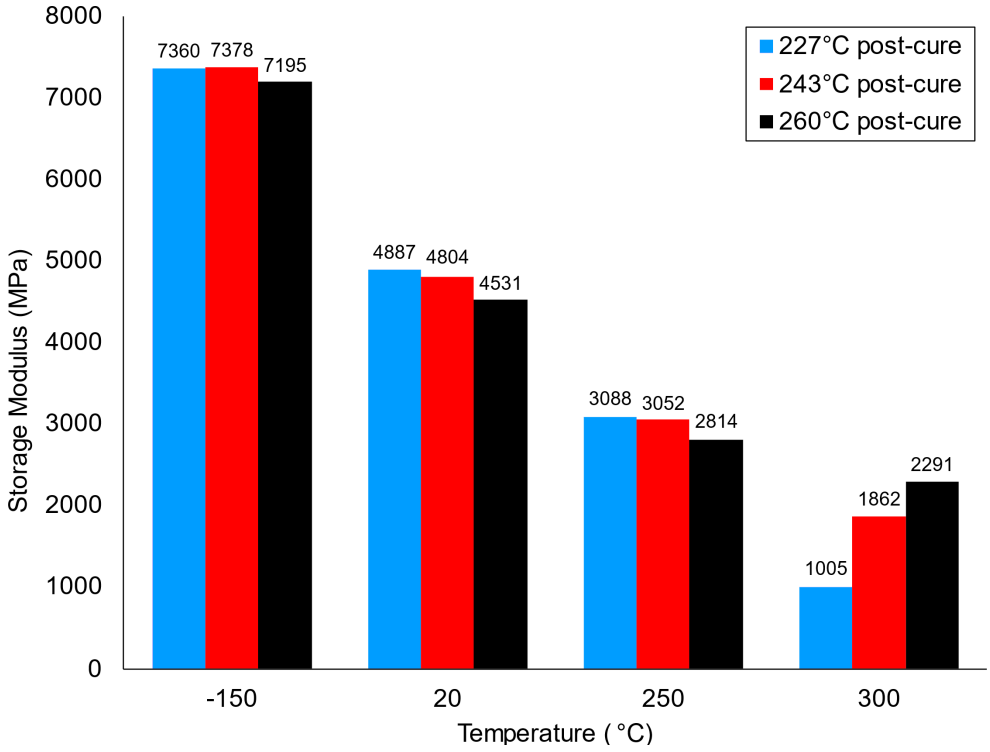

Figure 6: Storage modulus versus temperature for Cycom® 5250-4 after different post-cure conditions using 3-point-bending DMA test at10 Hz.

For an operating temperature of 300°C and a resin modulus of 2000 MPa, a 260°C post-cure condition can be used, as shown in Figure 6. The resin moduli at cryogenic temperatures were excellent for all three samples, exhibiting moduli greater than 7000 MPa at -150°C. In addition to the mechanical effects, higher post-cure temperatures had a visual effect where higher post-cure temperature tended to produce darker resin samples as shown in Figure 7 presumably because of further thermal degradation during post-cure.

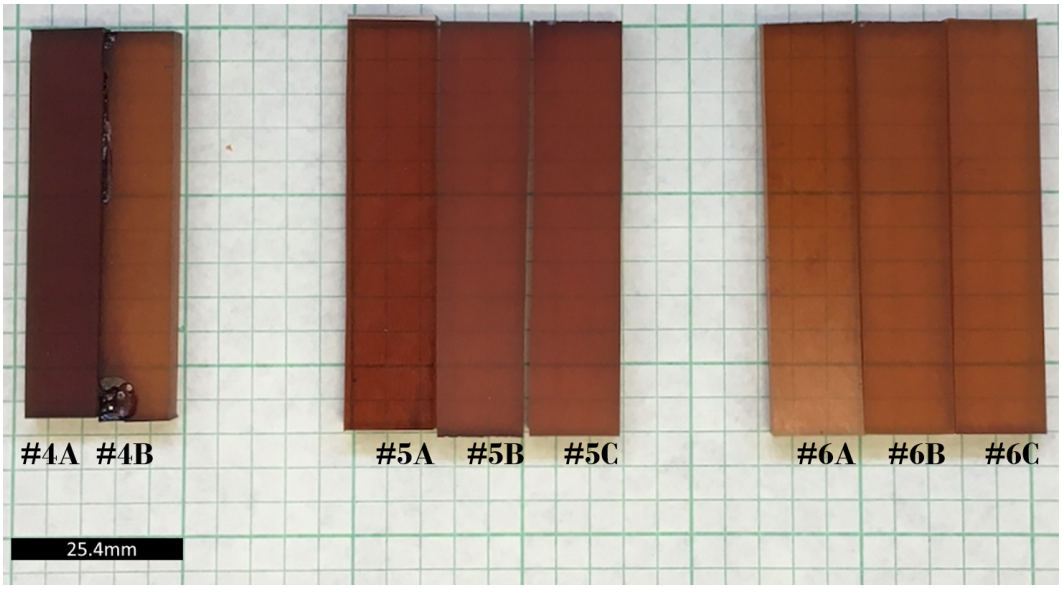

Figure 7: Specimens for DMA tests: # 4 Post-cured at 260°C, # 5 Post-cured at 243°C, # 6 Post-cured at 227°C. Note for a darker color for # 4A and # 5A; they were exposed to thermal heating from -155°C to 350°C at 5°C/min during DMA runs. Sample # 4B contains defects and was not used.

As shown in Figure 8, the BMI material experiences multiple peaks in loss modulus, one around -75°C, another broad hump around 100–130°C, and a third that corresponds closely with the T_g around 300°C. The sub-T_g transition near -75°C is likely related to a toughening mechanism of the toughened BMI. For determination of T_g, an automated process was used to find the onset T_g from the logarithmic graph of the storage modulus, as described in Appendix A.

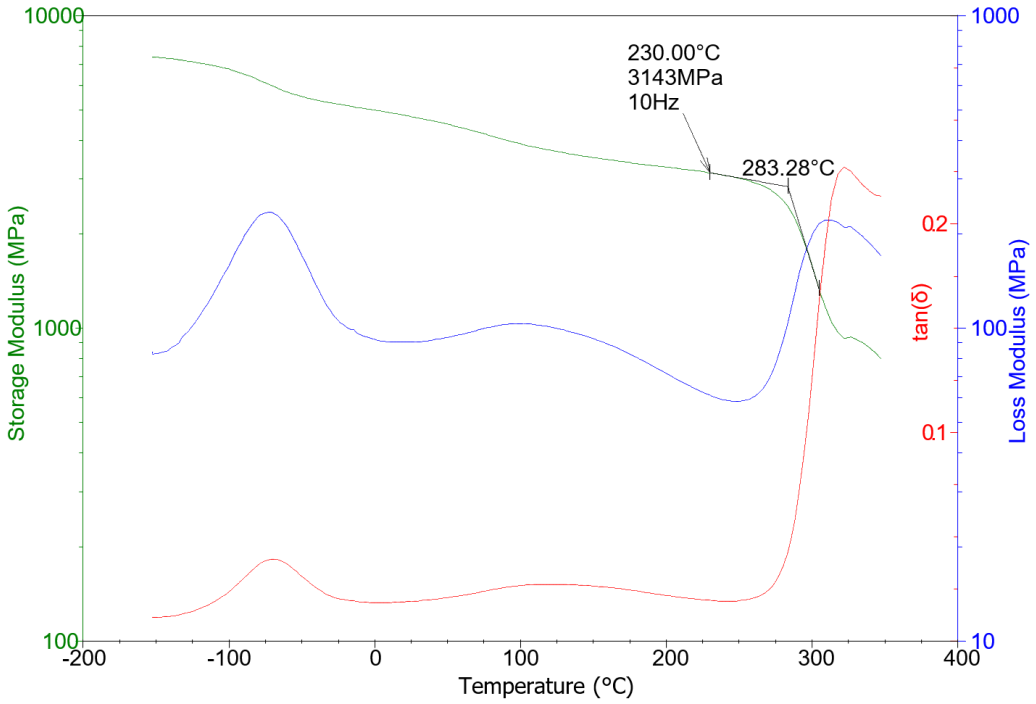

Figure 8: Measured storage modulus, loss modulus, and tan δ (where tan δ is the ratio of the loss and storage moduli [10]) for the 243°C post-cured sample.

3.2 Effects of thermal cycling

The effects of thermal cycling on the storage modulus as a function of temperature for the three different post-cure temperatures are shown in Figure 9. The lightly colored bands indicate the uncertainty (variation during 10 cycles) in each measurement. The modulus data at selected thermal cycles of # 1, # 2, # 5, and # 10 under the post-cure condition of 260°C are shown in Figure 10. In Figure 10, it is shown that increased cycling tends to reduce modulus at temperatures lower than 50°C while increasing modulus at temperatures higher than 50°C. As the cycling tests were run only with temperature ranges below the T_g (in order to prevent warping of the sample during the test) and below the 250°C to 290°C temperature range, the increased post-cure temperature decreased the modulus of post-cured BMI samples, as shown in Figures 4 and 10.

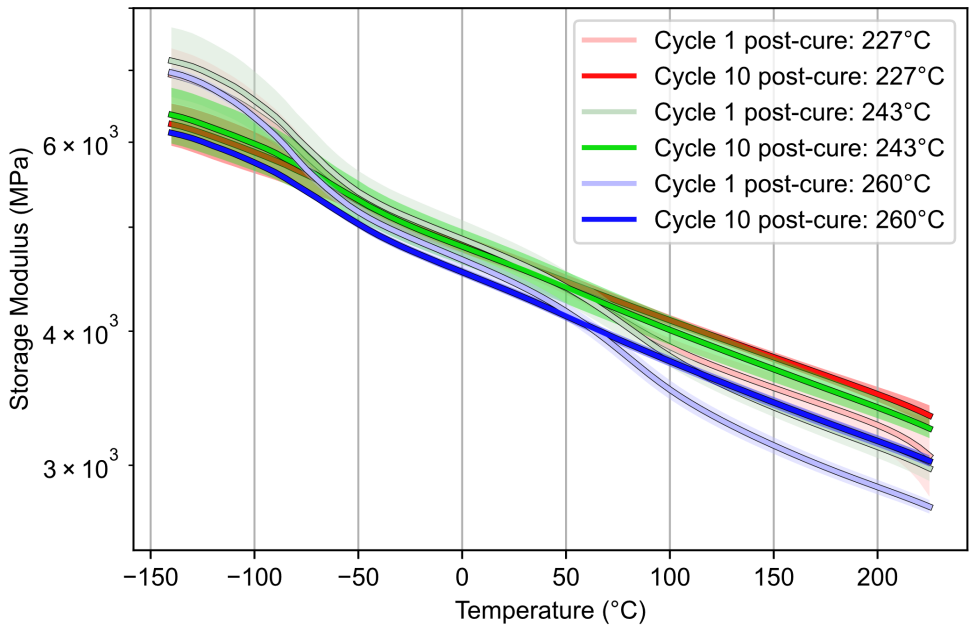

Figure 9: Cycling tends to reduce the effects seen of post-cure heat treatment, in both directions. Light-colored bands represent uncertainty of about one standard deviation.

As can be seen in Figures 9 and 10, cycling reduced the modulus at low temperatures (especially below -80°C) but increased it at high temperatures (above approximately 60°C).

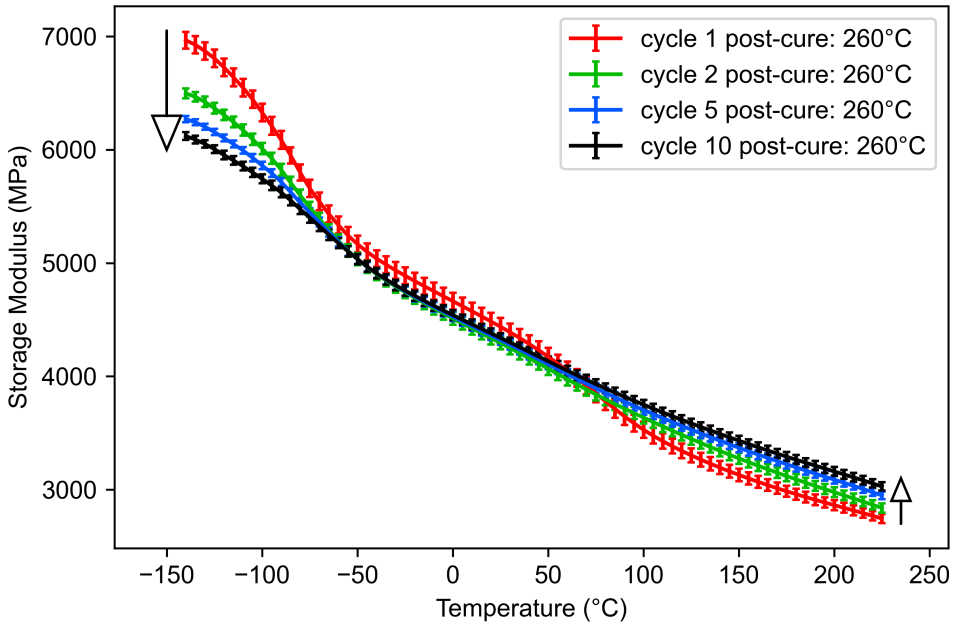

Figure 10: Storage modulus versus temperature measured by DMA over multiple thermal cycles. 260°C post-cure condition. Error bars represent about one standard deviation of data spread based on repeated experiments.

4 Conclusion

By the use of an elevated post-cure temperature according to the manufacturer's recommendation, BMI resin can be suitable for an application requiring service at both high and low temperatures corresponding to the temperature extremes a liquid rocket engine combustion chamber may see in service. DMA measurement indicated that a higher post-cure temperature increases T_g, causes the onset of modulus to drop, and reduces overall storage modulus. A consistent method of measuring glass transition was developed, which can improve future tests. Additional mechanical tests (such as short beam shear or tensile strength tests) may be needed to determine the suitability of BMI in a specific temperature regime, and composite samples may need to have these tests run under cycling conditions. The DMA testing confirmed that, as expected, the T_g increased with higher post-cure temperatures, but this improvement came at the expense of a slight reduction of modulus at all temperatures lower than the T_g onset. Further DMA testing which cryogenically cycled the neat resin samples demonstrated that such thermal cycling tended to reduce modulus at lower temperatures but increase it slightly at higher temperatures. Suggested future work includes comparison with tensile-mode film samples, different resin compositions, and composite samples.

References

1. J. Fikes, "Space technology mission directorate: Game changing development program: Rapid Analysis and Manufacturing Propulsion Technology (RAMPT)," tech. rep., 2018.

2. G. F. Limbrunner and L. Spiegel, *Applied statics and strength of materials*. Pearson Prentice Hall, 1998.

3. G. P. Sutton, *Rocket propulsion elements: an introduction to the engineering of rockets*. John Wiley&Sons, fifth ed., 1986.

4. C. Maruyama, "Scorpius 20k lbf engine," Jun 2023. https://scorpius.com/scorpius-20k-lbf-engine/.

5. "Standard test method for glass transition temperature (DMA Tg) of polymer matrix composites by dynamic mechanical analysis (DMA)," No. ASTM D7028-07(2015), ASTM West Conshohocken, PA, 2015.

6. "Standard test method for assignment of the glass transition temperature by dynamic mechanical analysis," No. ASTM E1640-18, ASTM West Conshohocken, PA, 2018.

7. Y. Li, *Synthesis and cure characterization of high temperature polymers for aerospace applications*. Texas A&M University, 2004.

8. E. E. Shin, R. J. Morgan, J. Zhou, J. Lincoln, R. Jurek, and D. B. Curliss, "Hygrothermal durability and thermal aging behavior prediction of high-temperature polymer-matrix composites and their resins," *Journal of thermoplastic composite materials*, vol. 13, no. 1, pp. 40–57, 2000.

9. "Electrical insulating materials - Methods of test for the determination of the glass transition temperature," No. IEC 61006:2004, International Electrotechnical Commission, 2004.

10. J. R. Fried, *Polymer science and technology*. Pearson Education, 1995.

Appendix A

Supplemental information on DMA frequency dependence.

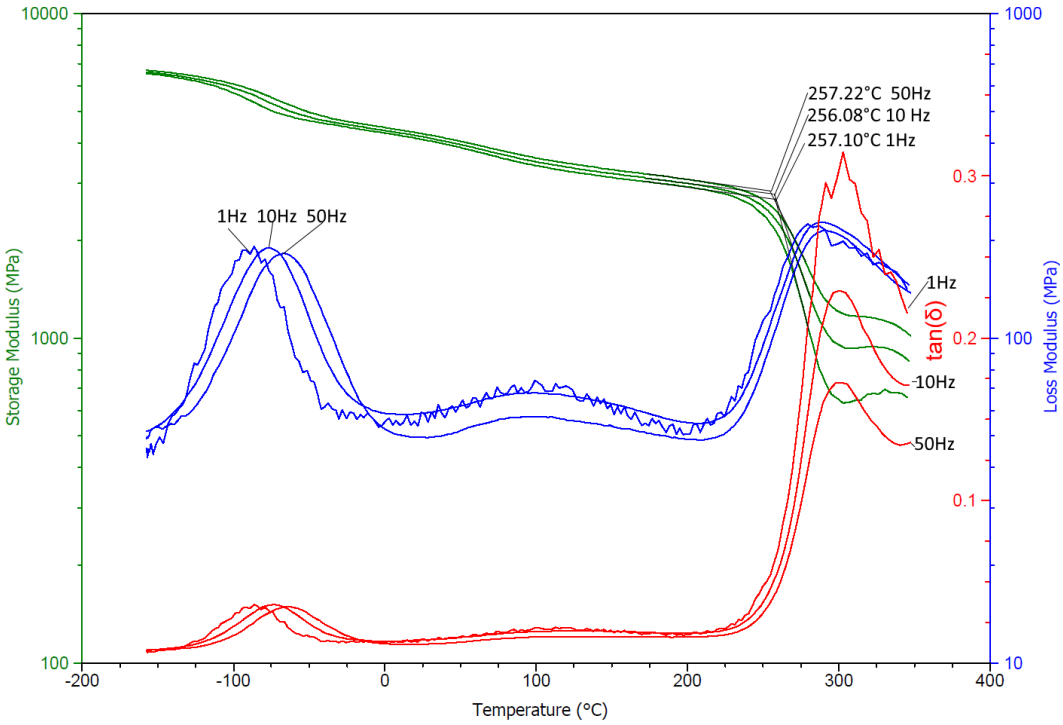

Figure A1: Storage modulus, loss modulus, and tan δ versus temperature measured by DMA over multiple thermal cycles. 227°C post-cure condition.

Appendix B

Interpretation of glass transition temperature.

Glass transition temperature is a range of values of temperature where the material transitions from a glassy state to a rubbery state. The temperature region in between is the glass transition region, as in Figure B1.

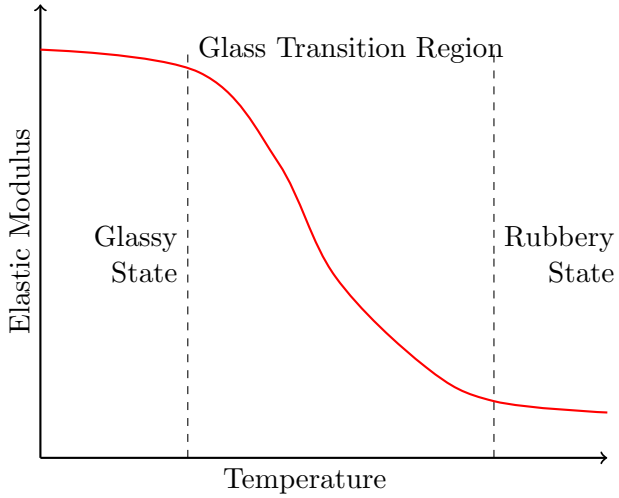

Figure B1: Representative curve used for interpreting the glass transition temperature from a plot of elastic modulus versus temperature.

As noted in measurement standards ASTM E1640 and D7028, there are three main ways to determine glass transition temperature using the data produced through DMA tests. One is by plotting the intersecting point of two lines drawn from constant-slope region: immediately before the T_g (in an area of the curve where the slope is constant) and then another line in the inflection region, for a graph of the storage modulus. The temperature at which these two points intersect is the T_g onset point. Another method to determine T_g is to draw the peak of the loss modulus. The third is the peak of the tanδ curve. These methods of determining T_g are slightly different from one another, and so it is necessary to decide on a consistent value. The storage modulus slope line coincidence method tends to give the lowest value of T_g, i.e. the earliest point at which the material is transitioning to a rubbery state. As the purpose of our analysis is, in part, to determine the usability of this resin system at high temperatures, it is desired to find the earliest point when the material can be said to have become no longer glassy. Therefore, the storage modulus slope line coincidence method will be used in this paper. One consideration with the storage modulus slope line coincidence method is that the exact procedure to measure it can be slightly subjective as exactly where to draw the slope from can vary slightly from researcher to researcher or it may depend on the software used. Sometimes the graph may be plotted linearly, which will produce

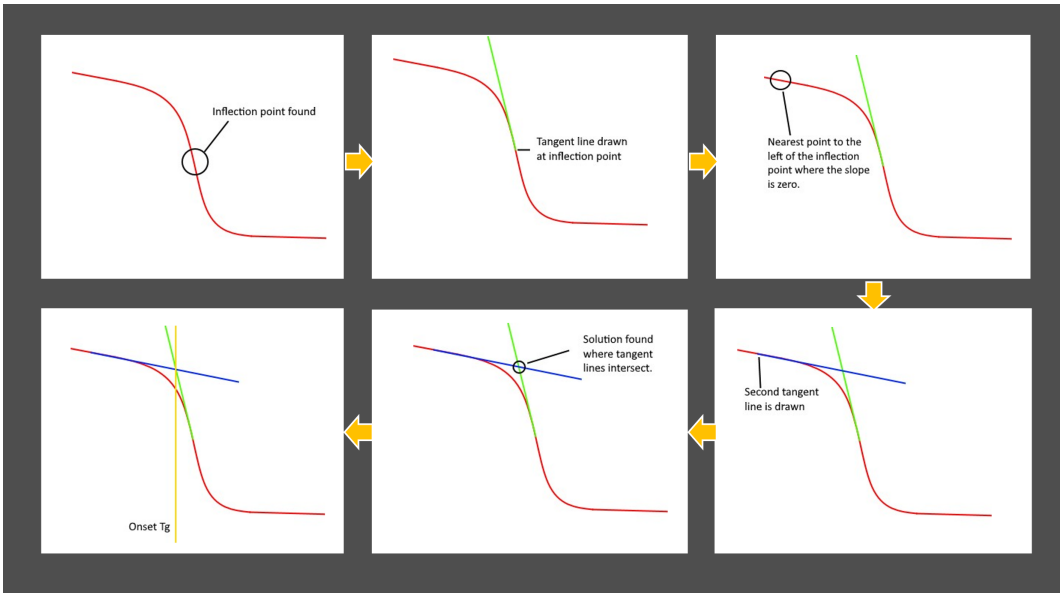

Figure B2: Step by step process for finding the T_g.

slightly different results from when the graph is drawn with the storage modulus plotted on a logarithmic scale. Logarithmic scale is the method used in this paper.

To eliminate the subjectivity in this kind of method, a procedure was used to find the tangent lines. For the tangent line in the inflection region, the point where the slope of the graph was most-negative was found by taking the second derivative of the logarithm of the storage modulus with respect to temperature and solving for points where it is zero:

$$\frac{\mathrm{d}^2 \log_{10} E'}{\mathrm{d}T^2} = 0 \tag{B1}$$

There are multiple such solutions to this, so the solution which corresponds to the most negative slope is chosen. A tangent line at that point was drawn by fitting a line to nearby points. A second tangent line was drawn in the same manner at the right-most point (but to the left of the found inflection region) where the second derivative of the logarithm of the storage modulus was equal to zero (i.e. where the slope of the graph was constant). In this way, as in Figure B2 the onset T_g could be found without the usual subjectivity associated with this approach.

This allows the onset T_g to repeatedly be found without subjective user error. Results are similar to using a full Thermal Analysis suite. The results on the left are with the automated approach above whereas the ones on the right are measured manually in Thermal Analysis software, as in Figure B3.

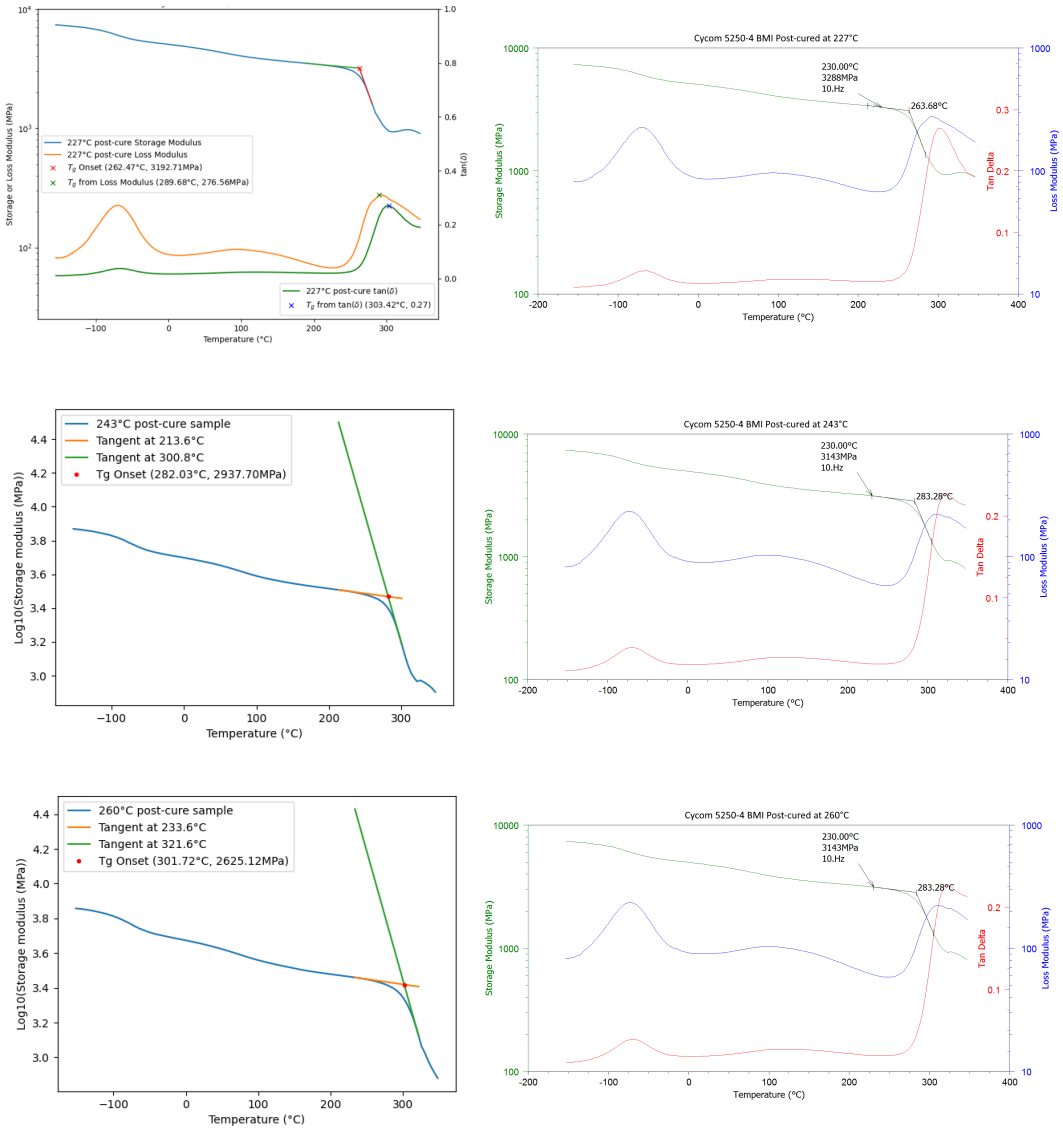

Figure B3: Automated (left) versus manual (right) finding of the T_g value for three different post-cure conditions.